On Performance Bounds for Space–Time Codes on Fading Channels

André P. des Rosiers, *Member, IEEE,* and Paul H. Siegel, *Fellow, IEEE*

***Abstract*—We evaluate truncated union bounds on the frame-error rate (FER) performance of space–time (ST) codes operating over the quasi-static fading channel and compare them with computer simulation results. We consider both ST trellis and block codes. We make the following contributions. For the case of ST trellis codes, we develop a general method, which we denote as *measure spectrum* analysis, that characterizes ST codeword differences and accommodates the combined influences of the ST code and channel scenario. We propose a numerical bounding method that converges in the measure spectrum to within a very small fraction of a decibel to the simulated FER over the full range of signal-to-noise ratio. In addition, we demonstrate the existence of *dominant* quasi-static fading error events and detail a method for predicting them. Using only this set of dominant measure spectrum elements, very rapid and tight numerical estimation of FER performance is attained.**

***Index Terms*—Block fading, distance spectrum, diversity, frame-error rate (FER), outage probability, performance bounds, quasi-static fading, space–time (ST) codes, union bound.**

I. Introduction

MULTIANTENNA communications on fading channels has been theoretically demonstrated to provide significant improvements in spectral efficiencies to a level that cannot be achieved by any other current method [1], [2]. Space–time (ST)-coded modulation, as introduced in [3]–[5], is a means of exploiting this gain in capacity by imposing a spatio–temporal structure onto the transmitted signal by allocating different symbols to different antennas. This structure is designed to guarantee a particular level of transmitter diversity, and to provide forward-error correction capability when communicating over fading channels.

In most cases of ST coding, the focus is on low-delay applications, thus coding is only performed within a block or frame of data, since coding across frames introduces delay. The appropriate channel property is the information outage probability [1], [6], which is a measure of the percentage of time that the instantaneous mutual information is below the code transmission rate. As noted by [7] and [8], the outage probability is closely related to the frame-error rate (FER). It was shown that in the limit, as the block length increases, the FER approaches the outage probability. In addition, the FER is reasonable as a means of comparison, since in many block-oriented systems, such as packet data communications, corrupted frames are discarded and a frame retransmission is requested.

The classical method of predicting code FER performance uses a truncated union bound on the probability of error as a function of the signal-to-noise ratio (SNR), and is calculated by summing the pairwise error probabilities (PEP) averaged over the channel for all codeword pairs. In [3] and [4], the analysis of an upper bound on the PEP identified some of the structural properties that govern code performance over fading channels. This has led to code construction methods that exploit these properties [9]–[14]. A general method for computing the ST PEP for channels with different degrees of spatial and temporal correlation was presented in [15] and [16].

In Sections II and III, we define the general system model used throughout this paper, and provide a derivation of the PEP and related bounds. Although PEP analysis is richly covered in the literature, [17]–[19], we provide additional insights, such as a generalization of the exact PEP equation in order to accommodate an arbitrary number of receive antennas and different channel types.

To evaluate the union bound for specific codes, the pairwise codeword differences must be characterized according to an appropriate performance measure for the given channel model. The definition of this measure is dependent upon the channel. Enumeration of the codeword-difference measures and their multiplicities is analogous to the classical code-distance spectrum. In Section III, we generalize to ST trellis codes the distance-spectrum-evaluation methods in [20], in order to accommodate the performance measures for arbitrary channel types such as additive white Gaussian noise (AWGN), independent Rayleigh fading, and quasi-static Rayleigh fading. Our work deals primarily with channels without memory. However, channels with memory, such as frequency-selective fading channels, can be accommodated by concatenating the channel and code at a cost of higher computational complexity. We call this error-event enumeration process *measure spectrum* analysis, since in the general case, the measure is not a true distance in a mathematical sense. Other authors have demonstrated techniques that compute a small number of ST error events [21], [22], however, our method computes all error events in

Paper approved by N. Al-Dhahir, the Editor for Space–Time, OFDM, and Equalization of the IEEE Communications Society. Manuscript received March 28, 2003; revised July 18, 2003 and January 7, 2004. This work was supported in part by Intersil Corporation, in part by the University of California under UC CoRe Grant C98-07, and in part by the National Science Foundation under Grant NCR-9612802. This paper was presented in part at the International Symposium on Information Theory and its Applications, Honolulu, HI, November 2000, and in part at the International Conference on Communications, Anchorage, AK, May 2003.

A. P. des Rosiers is with the Radar Division, Adaptive Processing Section, Code 5312, Naval Research Laboratory, Washington, DC 20375-5312 USA (e-mail: desrosiers@nrl.navy.mil).

P. H. Siegel is with the Center for Magnetic Recording Research, University of California, San Diego, La Jolla, CA 92093-0401 USA (e-mail: psiegel@ucsd.edu).

Digital Object Identifier 10.1109/TCOMM.2004.836429

an arbitrary number of trellis steps. We also demonstrate in Section III a method for performing measure spectrum analysis for ST block codes.

Conventional truncated union-bounding techniques based on exact PEPs are not adequate for predicting ST-coded performance in quasi-static fading, as they do not converge as the number of measure spectrum elements is increased in the bound computation [23]. We deal with this problem in [16], which was the first to generalize the numerical "limit-before-averaging" bounding techniques of [23] to ST codes in quasi-static fading. In [23], this numerical bounding method was shown to provide for convergence in the measure spectrum, and offer a significantly tighter bound for convolutional codes used on parallel (non-cross-coupled) quasi-static fading channels. We discovered in [16] that these properties also hold for ST codes operating over quasi-static fading channels. Many subsequent authors have independently used this method in their analysis of ST trellis codes [24]–[26]. However, as we demonstrated in [16] and [27], this improved bound has two significant additional properties. First, not only does this bound converge in the measure spectrum, but it also is very tight, converging within a very small fraction of a decibel (dB) to the simulated FER over the full range of SNR. Second, this convergence property appears to be due to a small set of *dominant error events*, and is a function of the frame length. Because the conventional union bound does not converge in the measure spectrum for quasi-static fading, it is generally thought that dominant error events do not exist [23]. However, we demonstrate in Sections IV and V a method for predicting the dominant error events from the measure spectrum, and show that we can tightly bound the simulated FER performance with only this dominant set of two to three error events. We find that these properties hold for a wide sampling of ST trellis and block codes. Thus, for realistic block lengths, this numerical bounding method coupled with this small set of dominant error events results in a very rapid method for estimating ST code FER performance.

II. System Model

We consider a ST-coded system that employs L transmit antennas and M receive antennas. All L transmit antennas are assumed to be spatially uncorrelated. The baseband symbol derived from a constellation with unit average energy is transmitted by antenna i during time epoch n with average symbol energy E_s, and is denoted by $\sqrt{E_s}d_i(n)$. A codeword spans N time epochs, and during each time slot, L symbols are simultaneously transmitted from the L transmit antennas. In this paper, N represents the frame length, and $N \cdot L$ is the number of symbols transmitted during a block. Each receive antenna observes a noisy superposition of the L transmitted symbols impaired by a multiplicative distortion $\gamma_{ij}(n)$, between transmit antenna i and receive antenna j at time epoch n. The complex fading values $\gamma_{ij}(n)$ follow a known probability law, and are often modeled as samples from a Gaussian random process.

After matched filtering, the sampled received signal at receive antenna j for a frame length of N is

$$r_j(n) = \sqrt{E_s}\sum_{i=1}^{L} d_i(n)\gamma_{ij}(n) + \eta_j(n), \quad j = 1,\ldots,M; \quad n = 1,\ldots,N \tag{1}$$

where $\eta_j(n)$ is zero-mean additive complex Gaussian noise with complex variance N_o. Expression (1) can be placed in matrix form after defining a suitable representation for the codeword matrix. For one possible structure [15], given a single receive antenna $j = 1$, a codeword a of code $\mathcal{C}$, denoted $\tilde{\mathbf{D}}_a = [\mathbf{D}_a(1),\ldots,\mathbf{D}_a(L)]$, is defined as an $N \times LN$ block matrix, where each $\mathbf{D}_a(i)$ is an $N \times N$ diagonal codeword matrix of complex constellation symbols $d_i(n)$. A system with M spatially uncorrelated receive antennas is modeled as an $MN \times MLN$ block diagonal codeword matrix

$$\mathbf{D}_a = \mathrm{diag}(\tilde{\mathbf{D}}_a,\ldots,\tilde{\mathbf{D}}_a).$$

Given the definition of $\mathbf{D}_a$, (1) in matrix form becomes

$$\mathbf{r} = \sqrt{E_s}\mathbf{D}_a\boldsymbol{\gamma} + \boldsymbol{\eta}$$

where $\mathbf{r} = [r_1(1),\ldots,r_1(N),\ldots,r_M(1),\ldots,r_M(N)]^{\mathrm{T}}$ and $\boldsymbol{\eta} = [\eta_1(1),\ldots,\eta_1(N),\ldots,\eta_M(1),\ldots,\eta_M(N)]^{\mathrm{T}}$ are vectors of length MN, and $\boldsymbol{\gamma} = [\boldsymbol{\gamma}_{1,1}^{\mathrm{T}},\ldots,\boldsymbol{\gamma}_{L,1}^{\mathrm{T}},\ldots,\boldsymbol{\gamma}_{1,M}^{\mathrm{T}},\ldots,\boldsymbol{\gamma}_{L,M}^{\mathrm{T}}]^{\mathrm{T}}$ with $\boldsymbol{\gamma}_{i,j} = [\gamma_{i,j}(1),\ldots,\gamma_{i,j}(N)]^{\mathrm{T}}$ is a stacked vector of length MLN where superscript $^{\mathrm{T}}$ indicates transposition.

III. ST PEP

A. Probability of Error

Assuming the receiver has perfect knowledge of the channel fading coefficient vector $\boldsymbol{\gamma}$, the conditional probability of incorrectly decoding the transmitted codeword matrix is upper bounded by the classical union bound $\mathrm{P}_{\mathrm{ub}}(e|,\boldsymbol{\gamma})$ and satisfies [28]

$$\mathrm{P}(e|\boldsymbol{\gamma}) \le \mathrm{P}_{\mathrm{ub}}(e|\boldsymbol{\gamma}) \stackrel{\mathrm{def}}{=} \frac{1}{|\mathcal{C}|}\sum_{\mathbf{D}_a\in\mathcal{C}}\sum_{\mathbf{D}_b\in\mathcal{C},\mathbf{D}_b\neq\mathbf{D}_a}\mathrm{P}(\mathbf{D}_a \to \mathbf{D}_b|\boldsymbol{\gamma}) \tag{2}$$

where the summation is performed over all conditional PEPs, $\mathrm{P}(\mathbf{D}_a \to \mathbf{D}_b|\boldsymbol{\gamma})$, in code $\mathcal{C}$ of choosing codeword $\mathbf{D}_b$ instead of the transmitted codeword $\mathbf{D}_a$, given $\boldsymbol{\gamma}$. In addition, $\mathrm{P}(\mathbf{D}_a \to \mathbf{D}_b|\boldsymbol{\gamma})$ assumes that $\mathbf{D}_b$ and $\mathbf{D}_a$ were the only two possible decoder outcomes. The conditional PEP is defined as [3]

$$\mathrm{P}(\mathbf{D}_a \to \mathbf{D}_b|\boldsymbol{\gamma}) = \mathcal{Q}\left(\sqrt{\frac{E_s}{2N_o}g(\mathbf{D}_{ba},\boldsymbol{\gamma})}\right) \tag{3}$$

where $\mathbf{D}_{ba} \stackrel{\mathrm{def}}{=} \mathbf{D}_b - \mathbf{D}_a$ is the codeword difference matrix, and $g(\mathbf{D}_{ba},\boldsymbol{\gamma}) = \boldsymbol{\gamma}^{\mathrm{H}}\mathbf{C}_{ba}\boldsymbol{\gamma}$ is the channel quadratic form and the Gram matrix $\mathbf{C}_{ba} \stackrel{\mathrm{def}}{=} \mathbf{D}_{ba}^{\mathrm{H}}\mathbf{D}_{ba}$ (conjugate transpose is denoted by superscript $^{\mathrm{H}}$). We also use the Gaussian tail function

$\mathcal{Q}(x) = (1/\sqrt{2\pi})\int_x^\infty \mathrm{e}^{-\theta^2/2}d\theta, x \geq 0$. If M multiple independent receive antennas are used, then the conditional PEP in (3) can be written as

$$Q\left(\sqrt{\frac{E_s}{2N_o}\sum_{j=1}^{M}\boldsymbol{\gamma}_j^{\mathrm{H}}\mathbf{C}_{ba}\boldsymbol{\gamma}_j}\right)$$

where $\boldsymbol{\gamma}_j$ is the jth independent realization of the fading vector, and $j = 1, \ldots, M$.

We now assume the complex fading coefficient from transmit antenna i to receive antenna j at time $n, \gamma_{ij}(n)$ is modeled as a zero-mean complex Gaussian random variable with unit complex variance. To obtain a closed-form expression for the average PEP, $\mathrm{P}(\mathbf{D}_a \rightarrow \mathbf{D}_b)$, we average (3) over the probability density function (PDF) of the quadratic form of complex Gaussian variates $g(\mathbf{D}_{ba}, \boldsymbol{\gamma})$, which can be written ([29, eqs. 14-4-13 and 14-5-26]

$$p_g(g) = \begin{cases} \sum_{l=1}^{R}\frac{A_l}{\lambda_l}\mathrm{e}^{-g/\lambda_l}, & \lambda_1 \neq \lambda_2 \neq \cdots \neq \lambda_R \\ \dfrac{1}{\lambda^R(L-1)!}g^{R-1}\mathrm{e}^{-g/\lambda}, & \lambda_1 = \lambda_2 = \cdots = \lambda_R = \lambda \end{cases} \quad (4)$$

where $A_l = \prod_{k=1,k\neq l}^{R}(\lambda_l)/(\lambda_l - \lambda_k)$ and the λ_l are the R nonzero eigenvalues of the matrix product $\mathbf{C}_{\boldsymbol{\gamma}}\mathbf{C}_{ba}$, denoted as $\lambda_l(\mathbf{C}_{\boldsymbol{\gamma}}\mathbf{C}_{ba})$. Expression $\mathbf{C}_{\boldsymbol{\gamma}} = \mathrm{E}\{\boldsymbol{\gamma}\boldsymbol{\gamma}^{\mathrm{H}}\}$ is the $MLN \times MLN$ channel covariance matrix. We also note that R is the rank of $\mathbf{C}_{\boldsymbol{\gamma}}\mathbf{C}_{ba}$ and is upper bounded by $R \leq M \cdot \min(L, N)$. E denotes the expectation operator. It is not difficult to show that the mean of g is $\mathrm{E}(g) = \sum_{l=1}^{L}\lambda_l = \mathrm{tr}(\mathbf{C}_{\boldsymbol{\gamma}}\mathbf{C}_{ba})$ where $\mathrm{tr}(\mathbf{A})$ is the trace of matrix $\mathbf{A}$.

Averaging (3) over the two cases in (4), the exact closed-form PEP expression is [29, eqs. 14-4-15 and 14-5-28], [30], shown in (5) at the bottom of the page, where $z_l = \sqrt{(E_s\lambda_l/(4N_o))/(1 + (E_s\lambda_l/(4N_o))}$. We emphasize that (4) and (5) are general, in terms of accommodating the combined influences of the ST code, number of receive antennas, and channel type on the exact PEP through the eigenvalues $\lambda_k(\mathbf{C}_{\boldsymbol{\gamma}}\mathbf{C}_{ba})$. This coupling of ST code and channel must be taken into account during code design and performance estimation.

Chernoff upper bounding (3) at high SNR gives the expression from [4], however, generalized for an arbitrary channel

$$\mathrm{P}(\mathbf{D}_a \rightarrow \mathbf{D}_b) \leq \left(\frac{E_s}{4N_o}\right)^{-R}\left[\left(\prod_{k=1}^{R}\lambda_k(\mathbf{C}_{\boldsymbol{\gamma}}\mathbf{C}_{ba})\right)^{\frac{1}{R}}\right]^{-R}. \quad (6)$$

From bound (6), we see that ST code design requires that both the rank R and the minimum geometric mean of the nonzero eigenvalues are maximized. These code-design requirements, first identified in [4] as the rank and determinant criteria, respectively, characterize the diversity achieved and the point of low SNR rolloff. Since the nonzero eigenvalues of $\mathbf{C}_{\boldsymbol{\gamma}}\mathbf{D}_{ba}^{\mathrm{H}}\mathbf{D}_{ba}$ and $\mathbf{D}_{ba}\mathbf{C}_{\boldsymbol{\gamma}}\mathbf{D}_{ba}^{\mathrm{H}}$ are equivalent, we choose to define the *error-event matrix* (EEM) as

$$\tilde{\mathbf{C}}_{ba} \stackrel{\mathrm{def}}{=} \mathbf{D}_{ba}\mathbf{C}_{\boldsymbol{\gamma}}\mathbf{D}_{ba}^{\mathrm{H}}$$

which emphasizes the dependency of the ST error event on the channel characteristics. By specializing $\mathbf{C}_{\boldsymbol{\gamma}}$ for a particular channel scenario, we modify the structure of $\tilde{\mathbf{C}}_{ba}$ and, consequently, the measure on the error events, as we see in the following.

B. Computing the ST Trellis Code Measure Spectrum

For computing the ST measure spectrum, the union upper bound on the probability of error event (2) is further upper bounded by the union bound on the probability that an error event occurs at trellis epoch zero, also known as the probability of first error event [31]. We denote this bound by $\mathrm{P}_{\mathrm{ub}}(e_0|\boldsymbol{\gamma})$ and it is expressed as

$$\mathrm{P}_{\mathrm{ub}}(e|\boldsymbol{\gamma}) \leq \mathrm{P}_{\mathrm{ub}}(e_0|\boldsymbol{\gamma}) = \sum_{\substack{\mathbf{D}_a, \mathbf{D}_b \in \mathcal{C}(s_0) \\ \mathbf{D}_b \neq \mathbf{D}_a}} h(\mathbf{D}_a \rightarrow \mathbf{D}_b)\mathrm{P}(\mathbf{D}_a \rightarrow \mathbf{D}_b|\boldsymbol{\gamma}) \quad (7)$$

where $\mathcal{C}(s_0)$ is the set of codewords from code $\mathcal{C}$ starting in state s_0 at time zero from state-space $\mathcal{S}$, with total number of states $|\mathcal{S}|$. The number of branches emanating from each state (equivalently, the number of symbols in the modulation alphabet) is denoted by B. The average multiplicity $h(\mathbf{D}_a \rightarrow \mathbf{D}_b)$ is the number of error events $\mathbf{D}_a \rightarrow \mathbf{D}_b$ with the same EEM, $\tilde{\mathbf{C}}_{ba}$, and is scaled by $1/(|\mathcal{S}|B^k)$, the total number of possible first error events of the same length k. The performance measure on the error event described by $\tilde{\mathbf{C}}_{ba}$ is defined as $m(\tilde{\mathbf{C}}_{ba})$. We will demonstrate in Section IV the importance of defining $h(\mathbf{D}_a \rightarrow \mathbf{D}_b)$ as the multiplicity of the distinct EEMs, rather than the multiplicity of distinct measures $m(\tilde{\mathbf{C}}_{ba})$, since the individual EEMs will be used in the calculation of the numerical bound. A detailed equation for computing $h(\mathbf{D}_a \rightarrow \mathbf{D}_b)$ can be found in [20].

The set of tuples

$$\{[h(\mathbf{D}_a \rightarrow \mathbf{D}_b), \tilde{\mathbf{C}}_{ba}, m(\tilde{\mathbf{C}}_{ba})] : \mathbf{D}_a, \mathbf{D}_b \in \mathcal{C}(s_0), \mathbf{D}_b \neq \mathbf{D}_a\}$$

is obtained by traversing the trellis of the ST code of interest. In the following, we will denote this measure as m_n for the measure at trellis step n, or simply m when the trellis step is not informative. The enumeration of the error events is quantified according to the value of this performance measure. For example, the Euclidean distance is used as the performance measure for codes operating in AWGN. For the general channel case, (3) indicates that the eigenvalues of the EEM are essential

$$\mathrm{P}(\mathbf{D}_a \rightarrow \mathbf{D}_b) = \begin{cases} \frac{1}{2}\sum_{l=1}^{R}A_l(1 - z_l), & \lambda_l \neq \lambda_k \forall l \neq k \\ \left[\frac{1}{2}(1 - z_1)\right]^R \sum_{k=0}^{R-1}\binom{R-1+k}{k}\left[\frac{1}{2}(1 + z_1)\right]^k, & \lambda_1 = \lambda_2 = \cdots = \lambda_R \end{cases} \quad (5)$$

for computing the error events, and the bound in (6) suggests the product of these nonzero eigenvalues is the appropriate choice of performance measure.

Our method of enumerating a finite number of ST trellis error events that generates the *truncated measure spectrum* is discussed in [32]. This computer-search procedure is a generalization of a method described in [20] to a ST code and arbitrary channel. Since most of the ST trellis codes discussed in the literature do not comply with the classic symmetry conditions and are nonuniform, we must consider all possible pairwise codeword differences in computing the measure spectrum. Therefore, the complexity of this method grows with the square of the number of encoder trellis states. The algorithm considers all possible pairs of merged codeword paths by operating on a superstate trellis, denoted S_{mn}, with $|\mathcal{S}|^2$ superstates corresponding to all pairs of states in the original trellis. An error event in the original trellis, consisting of a pair of paths diverging from state σ_m and remerging into state σ_n, while sharing no intermediate states, corresponds to a path in the superstate trellis that starts in S_{mm} and ends in S_{nn}. For each superstate S_{mn}, we create a data structure which contains a set of arrays for storing the distinct partial EEM, measure, multiplicity, and number of bit errors of a running error event at each trellis epoch. Two stopping criteria are used to end the algorithm. The first stopping criterion advances through the trellis computing error events until all error events with measure less than or equal to the maximum desired measure $m_{\max}$ are found. The second stopping criterion finds all measures regardless of magnitude in $T_{\max}$ trellis steps, with $T_{\max} \leq N$.

All ST trellis codes, as defined in [4], can be considered as block codes of length N over the real numbers, since known symbols are used to terminate the trellis code to a known state. A complete measure spectrum for a terminated ST trellis code is found by computing the appropriate measure on all error events in N trellis epochs. As we step through the trellis, these channel-dependent measures are nondecreasing in error-event length for all the possible codeword paths. Thus, we expect the lowest values of measure in the initial epochs of the trellis. Given that the number of codeword matrices is $|\mathcal{C}| = |\mathcal{S}|B^N$, this search procedure can be computationally demanding. However, as we will show in the sequel, computing the full measure spectrum for a truncated ST trellis code is not always required, since a small set of error events from the initial trellis epochs appear to characterize the simulated FER.

We next give some examples of this general method of computing the ST measure spectrum for different channels of interest.

1) Example: AWGN Model: In AWGN, $\mathbf{C}_{\boldsymbol{\gamma}}$ is the all-ones matrix, which implies that we should sum the outputs of the transmit antennas at each time epoch. This specializes the EEM to $\tilde{\mathbf{C}}_{ba} = \tilde{\mathbf{d}}_{ba}\tilde{\mathbf{d}}_{ba}^{\mathrm{H}}$, where $\tilde{\mathbf{d}}_{ba} = [\sum_{i=1}^{L} d_i^{(ba)}(1), \ldots, \sum_{i=1}^{L} d_i^{(ba)}(N)]^{\mathrm{T}}$, and we denote the nonzero elements of matrix $\mathbf{D}_{ba}$ by $d_i^{(ba)}(n), i = 1, \ldots, L;\ n = 1, \ldots, N$. The single eigenvalue for the AWGN case is obtained by taking the trace of $\tilde{\mathbf{C}}_{ba}, \lambda(\tilde{\mathbf{C}}_{ba}) = \mathrm{tr}(\tilde{\mathbf{C}}_{ba}) = \tilde{\mathbf{d}}_{ba}^{\mathrm{H}}\tilde{\mathbf{d}}_{ba} = \sum_{n=1}^{N} |\sum_{i=1}^{L} d_i^{(ba)}(n)|^2$. It follows that the exact PEP in AWGN is $P(\mathbf{D}_a \rightarrow \mathbf{D}_b) = \mathcal{Q}(\sqrt{\mathrm{tr}(\tilde{\mathbf{C}}_{ba})(E_s/2N_o)})$. At each time epoch, we can compute the measure recursively as $m_n = |\sum_{l=1}^{L} d_l^{(ba)}(n)|^2 + m_{n-1}$.

2) Example: Independent Fading Model: In independent fading, each channel is spatially and temporally independent. This reduces $\mathbf{C}_{\boldsymbol{\gamma}}$ to the identity matrix, and the EEM simplifies to $\tilde{\mathbf{C}}_{ba} = \sum_{i=1}^{L} \mathbf{D}_{ba}(i)\mathbf{D}_{ba}^{\mathrm{H}}(i)$, where $\mathbf{D}_{ba}(i) = \mathbf{D}_b(i) - \mathbf{D}_a(i)$, and $\mathbf{D}_a(i)$ is defined in Section II. The nth eigenvalue of $\tilde{\mathbf{C}}_{ba}$ is $\lambda_n(\tilde{\mathbf{C}}_{ba}) = \|\mathbf{d}_{ba}(n)\|^2$, where $\mathbf{d}_{ba}(n) = [d_1^{(ba)}(n), \ldots, d_L^{(ba)}(n)]$ is the nth row of matrix $\mathbf{D}_{ba}$. The form of $\lambda_n(\tilde{\mathbf{C}}_{ba})$ permits the calculation of an eigenvalue at each successive epoch of an error event. Thus, at each time epoch, we compute $\lambda_n = \sum_{l=1}^{L} |d_l^{(ba)}(n)|^2$.

3) Example: Quasi-static Fading Model: For the case of quasi-static fading, the attenuation coefficients are constant over the duration of one codeword of N symbol epochs, i.e., $\gamma_{ij}(n) = \gamma_{ij}\ \forall i, j;\ n = 1, \ldots, N$. In quasi-static fading, $\mathbf{C}_{\boldsymbol{\gamma}}$ is a block diagonal matrix of $N \times N$ all-ones matrices. Thus, we can write the EEM as $\tilde{\mathbf{C}}_{ba} = \sum_{i=1}^{L} \mathbf{d}_i^{(ba)}\mathbf{d}_i^{(ba)\mathrm{H}}$ where $\mathbf{d}_i^{(ba)} = [d_i^{(ba)}(1), \ldots, d_i^{(ba)}(N)]^{\mathrm{T}}$. If we define the codeword matrix as $\hat{\mathbf{D}}_{ba} = [\mathbf{d}_1^{(ba)}, \ldots, \mathbf{d}_N^{(ba)}]$, the same expression for the EEM can be obtained by $\tilde{\mathbf{C}}_{ba} = \hat{\mathbf{D}}_{ba}\hat{\mathbf{D}}_{ba}^{\mathrm{H}}$ as in [30]. Since $\hat{\mathbf{D}}_{ba}\hat{\mathbf{D}}_{ba}^{\mathrm{H}}$ and $\hat{\mathbf{D}}_{ba}^{\mathrm{H}}\hat{\mathbf{D}}_{ba}$ have the same nonzero eigenvalues, we can redefine the expression for the EEM in quasi-static fading to be $\tilde{\mathbf{C}}_{ba} = \hat{\mathbf{D}}_{ba}^{\mathrm{H}}\hat{\mathbf{D}}_{ba}$, which can be computed using $\tilde{\mathbf{C}}_{ba} = \sum_{n=1}^{N} \tilde{\mathbf{C}}_{ba}(n)$, where $\tilde{\mathbf{C}}_{ba}(n) = \mathbf{d}_{ba}^{\mathrm{H}}(n)\mathbf{d}_{ba}(n)$ and $\mathbf{d}_{ba}(n) = [d_1^{(ba)}(n), \ldots, d_L^{(ba)}(n)]$. This expression suggests an efficient epoch-by-epoch approach to computing $\tilde{\mathbf{C}}_{ba}$, i.e., $\tilde{\mathbf{C}}_{ba}(n) = \mathbf{d}_{ba}^{\mathrm{H}}(n)\mathbf{d}_{ba}(n) + \tilde{\mathbf{C}}_{ba}(n-1)$. Also note that in this case $\tilde{\mathbf{C}}_{ba} = \hat{\mathbf{D}}_{ba}^{\mathrm{H}}\hat{\mathbf{D}}_{ba} = \mathbf{C}_{ba}$. The measure on $\mathbf{C}_{ba}$, denoted $m(\mathbf{C}_{ba})$, is the product of the nonzero eigenvalues and is computed after the error event has terminated. The trace of $\mathbf{C}_{ba}$ in quasi-static fading is important at low SNR and is computed as $\mathrm{tr}(\mathbf{C}_{ba}) = \sum_{n=1}^{N} \sum_{i=1}^{L} |d_i^{(ba)}(n)|^2$.

C. ST Measure Spectrum for Block Codes in Quasi-static Fading

We contrast the terminated trellis form of block code to ST block codes, which have a different codeword definition, but can be cast into the traditional block-code model. ST block codes, such as those based on orthogonal designs [33], are defined as a transmission matrix of size $n \times n$ with entries from a given modulation alphabet, where n usually equals the number of transmit antennas. For example, the Alamouti orthogonal design [5] has the form

$$\begin{bmatrix} d_1 & d_2 \\ -d_2^* & d_1^* \end{bmatrix}$$

where the d_k are two symbols from an r-phase-shift keying (PSK) or r-quadrature amplitude modulation (QAM) complex constellation. In order to compute the ST error events, we must compute the EEMs for all these distinct transmission matrices over a given constellation alphabet. For an alternative method, see [34].

The measure spectrum for ST block codes in quasi-static fading can be computed by comparing all possible distinct codeword matrices. The task is much simpler than the ST trellis code case, since we only have the equivalent of two

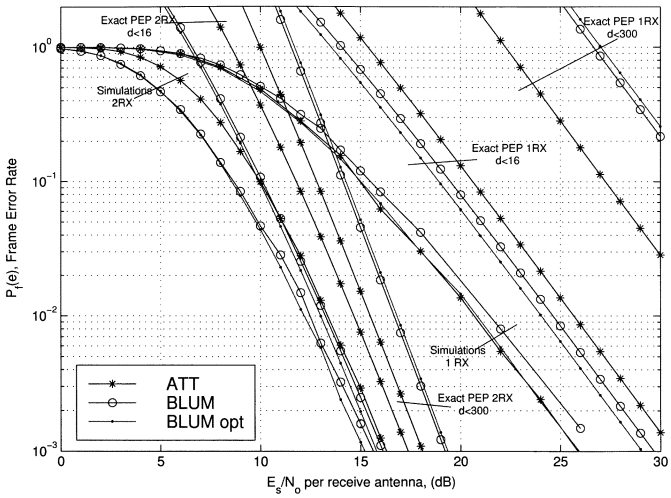

Fig. 1. FER quasi-static fading simulations and conventional union bounds using the exact PEPs of three 4-state, 4-PSK, $L = 2, M = \{1, 2\}, N = 130$ symbols. The PEP bounds are computed using all measures $m < 16$ and $m < 300$.

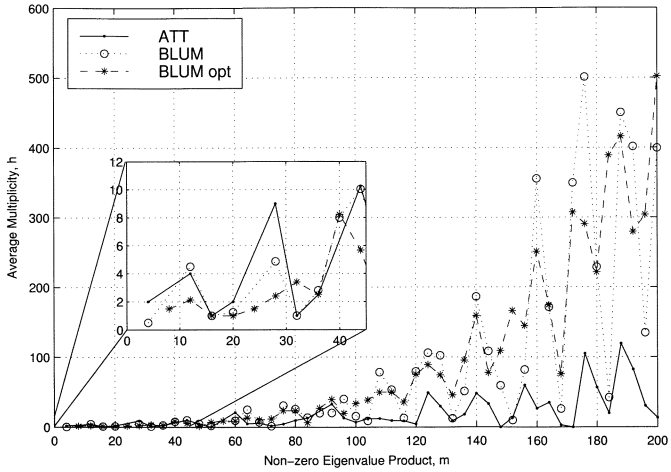

Fig. 2. Quasi-static fading measure spectrum for the three 4-state, 4-PSK, two transmit-antenna ST trellis codes.

states and n trellis iterations. Therefore, the multiplicity is scaled by $1/(|\mathcal{S}|B^n)$, where B is the number of symbols in the modulation alphabet and $|\mathcal{S}| = 2$. Suppose we transmit over N time epochs a ST block code containing n symbols from an r-PSK or r-QAM constellation. The rate of this system is then $R = (n/N)\log_2 r$ with $2^{RN} = r^n$ possible codeword matrices. Thus, the complexity of computing the measure spectrum grows rapidly, as larger transmission matrices are used and as the alphabet size increases. Fortunately, as we will show in the next section, this complexity can be reduced, since only a small number of error events contribute to accurately estimating the simulated quasi-static fading FER performance.

IV. Probability of Frame Error in Quasi-Static Fading

In this section, we derive a numerically computable upper bound for the FER of ST trellis and block codes in quasi-static fading that coincides empirically with the actual FER for the full range of SNR.

A. FER Upper Bounds

Upper bounds on the FER are

$$\mathrm{P_f}(e|\boldsymbol{\gamma}) \leq 1 - [1 - \mathrm{P_{ub}}(e_0|\boldsymbol{\gamma})]^N \tag{8}$$

$$\leq N \cdot \mathrm{P_{ub}}(e_0|\boldsymbol{\gamma}) \tag{9}$$

where a derivation for the first upper bound can be found in [31], and the second upper bound is obtained by expanding (8) as a binomial series and keeping only the first-order term.

B. Evaluation of the Conventional Union Bound on FER

We motivate the need for finding alternative bounding methods to the conventional union bound by observing the evaluation of the looser bound in (9) using the exact PEP equations in (5). In Fig. 1, we compare computer simulation to the loose FER bound in the presence of quasi-static Rayleigh fading of three 4-state, 4-PSK codes: the delay diversity code of [4, Fig. 4], an improved code found in [35, eq. (14)], and an "optimal" quasi-static fading code discussed in [10, Table I], denoted ATT, BLUM, and BLUM-opt, respectively. Analysis is performed with two transmit antennas, and one or two receive antennas. Now we denote the performance measure $m(\tilde{\mathbf{C}}_{ba})$ on the error event described by $\tilde{\mathbf{C}}_{ba}$ as m. We compare these simulations to two loose bounds based on (9) using the exact PEPs from (5). The first is computed with all measure spectrum elements having measure $m < 16$, and the second having all measures $m < 300$. The frame length is $N = 130$ symbols. For one receive antenna, simulations of the ATT and BLUM-opt display comparable behavior, providing a 1-dB improvement over the BLUM code at high SNR. However, the exact PEP bounds with $m < 16$ and $m < 300$ demonstrate conflicting performance outcomes, where the ATT has worst performance with $m < 16$, but the best, by far, when $m < 300$. This also indicates that the bounds do not converge as the number of code measure spectrum elements is increased, since we obtain progressively larger upper bounds. Similar observations can be made when comparing simulation results with computed bounds for two receive antennas. In summary, we observe that in this instance, it is difficult to predict relative performance gains using the exact PEP in the loose FER bound of (9).

To help explain this lack of convergence, we consider in Fig. 2 the quasi-static fading measure spectra multiplicity versus nonzero eigenvalue product of the three 4-state, 4-PSK, two transmit-antenna trellis codes. Because of the more complex structure of the two BLUM codes, we observe in these plots a more rapid exponential increase in their multiplicity over that of the simpler delay diversity ATT code. Clearly, if the corresponding PEPs in (5) do not decrease at rates larger than their multiplicities, then the conventional union bound will diverge.

C. Improved FER Bound in Quasi-Static Fading

We discuss here a bound that does converge as we increase the number of measure spectrum elements in the calculation of the FER bound. In the quasi-static fading case, all antennas, both

transmit and receive, are spatially independent. For ease of exposition, we modify the nomenclature. The ith EEM of the measure spectrum is denoted $\mathbf{C}_i = \mathbf{D}_i^{\mathrm{H}}\mathbf{D}_i$ with corresponding average multiplicity h_i, and the elements of the measure spectrum are ordered according to the measure of $\mathbf{C}_i$.

The main problem to overcome with the conventional union bound is that the first error-event probability for a particular fading vector realization may be larger than one. Any improved bounding method in quasi-static fading must limit the use of the union bound when it is unreliable. The authors in [23] used a truncation of the union bound before averaging over the fading probability distribution, for the case of convolutional codes over parallel channels. To extend this technique to ST codes over arbitrary channels, we substitute the conditional PEP (3) into the union bound (7), then into the tighter bound on FER (8). Then, we use a minimum function to prune the unreliable union bound realizations before averaging over the fading process [16]. Thus, for the FER, we obtain

$$\begin{aligned}\mathrm{P_f}(e) &\le 1 - \mathrm{E}_{\boldsymbol{\gamma}}\{[1-\min(1,\mathrm{P_{ub}}(e|\boldsymbol{\gamma}))]^N\}\\ &\approx 1 - \int_{\boldsymbol{\gamma}}\left[1-\min\left(1,\sum_{i=1}^{\mathcal{O}} h_i\mathcal{Q}(\sqrt{K\cdot\boldsymbol{\gamma}^{\mathrm{H}}\mathbf{C}_i\boldsymbol{\gamma}})\right)\right]^N \\ &\quad\cdot p_{\boldsymbol{\gamma}}(\boldsymbol{\gamma})d\boldsymbol{\gamma}\\ &\stackrel{\mathrm{def}}{=} \mathrm{FER}_{\mathcal{O}}(K) \end{aligned} \tag{10}$$

where the approximation in (10) is a result of the truncation of the measure spectrum to $\mathcal{O}$ distinct EEMs, $\mathbf{C}_i$, where $K = E_s/(2N_o)$ is the SNR, and $p_{\boldsymbol{\gamma}}(\boldsymbol{\gamma})$ is the multivariate PDF of $\boldsymbol{\gamma}$. Clearly, (10) exists since the minimum function bounds the integrand between zero and $p_{\boldsymbol{\gamma}}(\boldsymbol{\gamma})$. This integration can be performed numerically, using multidimensional Monte-Carlo integration methods by estimating $\mathrm{FER}_{\mathcal{O}}(K)$ by

$$\widehat{\mathrm{FER}}_{\mathcal{O}}(K) = \frac{1}{N_{\mathrm{samp}}}\sum_{k=1}^{N_{\mathrm{samp}}}\left[1-\min\left(1,\sum_{i=1}^{\mathcal{O}} h_i \times \mathcal{Q}\left(\sqrt{K\cdot\boldsymbol{\gamma}_k^{\mathrm{H}}\mathbf{C}_i\boldsymbol{\gamma}_k}\right)\right)\right]^N$$

where $\boldsymbol{\gamma}_k$ is the kth vector realization of N_{samp} realizations of the L-dimensional complex Gaussian random process with zero mean and unit complex variance elements.

The quadratic form in (10) can be expanded as

$$\begin{aligned}&\boldsymbol{\gamma}^{\mathrm{H}}\mathbf{C}_i\boldsymbol{\gamma}\\ &\quad= \sum_{m=1}^{L}\sum_{n=1}^{L}\gamma_m^* c_{mn}(i)\gamma_n\\ &\quad= \sum_{m=1}^{L} c_{mm}(i)|\gamma_m|^2 + 2\Re\left[\sum_{m=1}^{L}\sum_{n>m}^{L}\gamma_m^* c_{mn}(i)\gamma_n\right]\end{aligned}$$

where $[c_{mn}(i)], m,n \in \{1,\ldots,ML\}, c_{mn}\in\mathbb{C}$ are elements of the Gram matrix $\mathbf{C}_i = \mathbf{D}_i^{\mathrm{H}}\mathbf{D}_i$, and $\gamma_k, k = \{1,\ldots,ML\}$ are the independent complex Gaussian fade terms.

1) Analysis of the Improved FER Bound: As part of the analysis of the improved FER bound, we study the contribution of single error events to the overall bound. Let $z_s(K,\boldsymbol{\gamma}) = \sum_{i=1}^{s} h_i\mathcal{Q}(\sqrt{K\cdot\boldsymbol{\gamma}^{\mathrm{H}}\mathbf{C}_i\boldsymbol{\gamma}})$, and let a single term of $z_s(K,\boldsymbol{\gamma})$ be denoted $y = h\mathcal{Q}(\sqrt{Kg})$. The density of y is determined in the following proposition.

Proposition: Given the PDF $p_g(g)$ in (4) and the transformation $y = h\mathcal{Q}(\sqrt{Kg})$, we have for $p_y(y)$ (11), shown at the bottom of the page, where A_l is defined in (4) and λ_l are the R nonzero eigenvalues of matrix $\tilde{\mathbf{C}}_{ba}$. Also, $\mathcal{Q}^{-1}(y)$ is the inverse $\mathcal{Q}$-function and has the following definition:

$$\mathcal{Q}^{-1}(y) \stackrel{\mathrm{def}}{=} \begin{cases}\infty, & y<0\\ \sqrt{2}\mathrm{erf}^{-1}(1-2y), & 0\le y\le\dfrac{1}{2}\\ 0, & \dfrac{1}{2}<y\end{cases}$$

where $\mathrm{erf}^{-1}(y)$ is the inverse of the standard error function, $y = \mathrm{erf}(x) = (2/\sqrt{\pi})\int_0^x \mathrm{e}^{-t^2}dt$.

Proof: We note that $\mathcal{Q}(x)$ is monotonically decreasing for $x \ge 0$. Thus, we may transform the density using $p_y(y) = p_x(x=y)|(dx/dy)|$ where

$$\frac{dy}{dx} = -\frac{h}{\sqrt{2\pi}}\mathrm{e}^{-x^2/2}$$

and (11) follows. □

The mean of the quadratic form process, $p_g(g)$, is the sum of the eigenvalues of $\tilde{\mathbf{C}}_{ba}$. Since $p_y(y)$ is a transformation of $p_g(g)$, we expect $p_y(y)$ to have this same functional dependence on the eigenvalues. In Fig. 3, we plot $p_y(y)$ for two different constant nonzero eigenvalue products (determinant, in this case, since $\tilde{\mathbf{C}}_{ba}$ is assumed full rank), but vary the eigenvalues at an SNR of -2 dB for $L = 2$ transmit antennas and multiplicity $h = 2$. The mean for each of these densities is simply the exact PEP expression in (5) weighted by $h = 2$. For a given value of determinant, we observe that the density with the largest mean has identical eigenvalues. This behavior is a confirmation of the fact that the mean of the distributions is a function of the sum of the eigenvalues. Mathematically, this behavior is a consequence of the arithmetic-geometric mean (AMGM) inequality applied to the eigenvalues of positive definite matrices [36, eq. 7.8.1]. Since $p_y(y)$ is a function of $\mathrm{tr}(\tilde{\mathbf{C}}_{ba})$, given a particular value of determinant, the mean of process y is maximized when the sum of the eigenvalues is minimized. Thus, for fixed $\det(\tilde{\mathbf{C}}_{ba})$, by the AMGM inequality, $\det(\tilde{\mathbf{C}}_{ba}) \le [(1/L)\mathrm{tr}(\tilde{\mathbf{C}}_{ba})]^L$, and equality is achieved when the Gram matrix $\tilde{\mathbf{C}}_{ba}$ is diagonal with all diagonal elements equal to $(1/L)\mathrm{tr}(\tilde{\mathbf{C}}_{ba})$. We note that these eigenvalues of matrix $\tilde{\mathbf{C}}_{ba}$ are a function of the interactions

$$p_y(y) = \begin{cases}\displaystyle\sum_{l=1}^{R}\frac{A_l}{\lambda_l}\frac{2\sqrt{2\pi}}{hK}\mathcal{Q}^{-1}\left(\frac{y}{h}\right)\mathrm{e}^{-[\mathcal{Q}^{-1}(\frac{y}{h})]^2\frac{2-K\lambda_l}{2K\lambda_l}}, & \lambda_1\ne\lambda_2\ne\cdots\ne\lambda_R\\ \dfrac{2\sqrt{2\pi}}{h(K\lambda)^R(R-1)!}\left[\mathcal{Q}^{-1}\left(\dfrac{y}{h}\right)\right]^{2R-1}\mathrm{e}^{-[\mathcal{Q}^{-1}(\frac{y}{h})]^2\frac{2-K\lambda}{2K\lambda}}, & \lambda_1=\lambda_2=\cdots=\lambda_R=\lambda\end{cases} \tag{11}$$

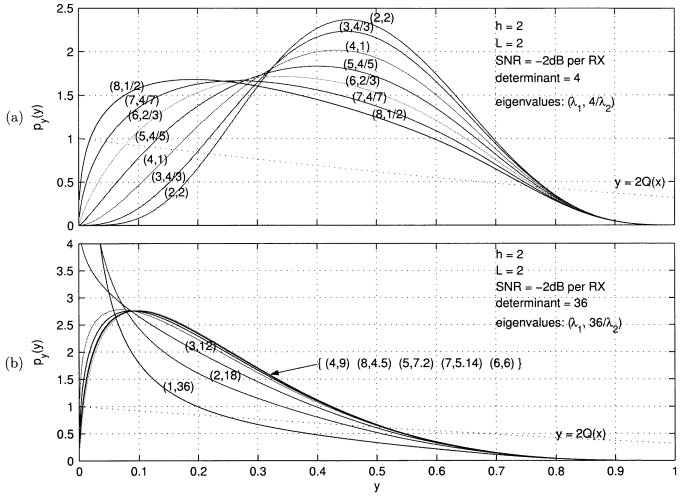

Fig. 3. Density function of $p_y(y)$ for $L = 2$ transmit antennas with multiplicity $h = 2$ at SNR $= -2$ dB. (a) Determinant $= 4$. (b) Determinant $= 36$.

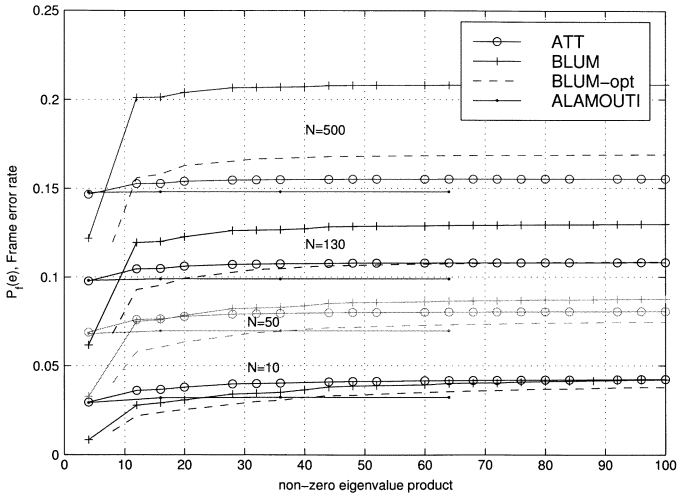

Fig. 4. Quasi-static fading ST convergence behavior. $\mathrm{FER}_{\mathcal{A}_k}(K)$ at $K = 15$ dB per receive antenna versus m_k of $\mathcal{A}_k = \{m_1, m_2, \ldots, m_k\}$ of four 4-PSK, $L = 2$, and $M = 1$ ST codes with $N = \{10, 50, 130, 500\}$.

among the ST code, number of receive antennas, and channel. The plots in Fig. 3 indicate that for the same multiplicity h, the EEM with smaller determinant and smaller trace, and correspondingly larger mean, will contribute more significantly to the overall density of $z_s(K, \boldsymbol{\gamma})$. This property of the eigenvalues for a single term of $z_s(K, \boldsymbol{\gamma})$ was arrived at from a different perspective and denoted as the equal eigenvalue criterion in [30], where this interaction between eigenvalue geometric mean and trace are exploited for optimal trellis-code design in quasi-static and independent fading.

V. Discussion and Results

In this section, we evaluate the tight upper bound on the FER for a sampling of ST trellis and block codes from the literature, and demonstrate that a small subset of quasi-static fading error events dominate the bound calculation.

We assume now that all EEMs for the codes of interest are full rank. Thus, for quasi-static fading, we use the determinant as the measure to classify EEMs: $m_i = \det(\mathbf{C}_i)$ for $i = 1, 2, \ldots, \mathcal{O}$, where $\mathcal{O}$ is the maximum measure index of interest. We let $\mathcal{A} = \{m_1, m_2, \ldots, m_{|\mathcal{A}|}\}$ be the set of all possible determinants of a given code of frame length N ordered such that $m_k < m_{k+1}$ for $k = 1, 2, \ldots, |\mathcal{A}| - 1$. Let $\mathcal{B} \subseteq \mathcal{A}$ be an arbitrary subset of $\mathcal{A}$. If $\mathcal{I}_{\mathcal{B}}$ denotes the set of indexes of all EEMs with determinants in the set $\mathcal{B}$, then

$$\mathrm{FER}_{\mathcal{B}}(K) = 1 - \int_{\boldsymbol{\gamma}} \left[1 - \min\left(1, \sum_{i \in \mathcal{I}_{\mathcal{B}}} h_i \mathcal{Q} \times \left(\sqrt{K \cdot \boldsymbol{\gamma}^{\mathrm{H}} \mathbf{C}_i \boldsymbol{\gamma}} \right) \right) \right]^N \cdot p_{\boldsymbol{\gamma}}(\boldsymbol{\gamma}) d\boldsymbol{\gamma}$$

is the partial FER computed with the determinant set $\mathcal{B}$ at SNR K. Now we let $\mathcal{A}_k = \{m_1, m_2, \ldots, m_k\}$ denote an ordered subset of $\mathcal{A}$, truncated to determinant $m_k \leq m_{|\mathcal{A}|}$. In Fig. 4, we evaluate $\mathrm{FER}_{\mathcal{A}_k}(K)$ for $k = 1, 2, \ldots, l$ where l is the index associated with the largest determinant of interest, and plot $\mathrm{FER}_{\mathcal{A}_k}(K)$ versus m_k, the maximum determinant in each set $\mathcal{A}_k$. For our examples in Fig. 4, the determinant set $\mathcal{A}$ includes all determinants less than or equal to 100. The saturation phenomenon of all the curves in Fig. 4 demonstrates the convergence behavior of the estimated FER of four ST 4-PSK codes with varying frame lengths at an SNR of 15 dB and one receive antenna. This convergence behavior is maintained even if the truncation length, quantified by the maximum measure, is increased. We make two critical observations. First, in all the codes considered, a small subset of *dominant error events* appears to contribute to the limit of the truncated bound. For short frame lengths, more error events contribute to the bound. However, the number of dominant error events is only two or three for longer, more realistic frame lengths. Table I lists the four dominant error events for these codes in quasi-static fading. Second, the relative value of the bounds is a function of the frame length. For example, when $N = 130$, the ATT and BLUM-opt codes

TABLE I
Dominant Error-Event Measures in Quasi-Static Fading, AWGN, and Independent Fading and Their Multiplicities for Four 4-PSK Codes and $N > 20$. Ordered in Decreasing Dominance

Code	Quasi. Fading		AWGN		Indep. Fading	
	$\prod_k \lambda_k$	Mult.	Trace	Mult.	$\prod_k \lambda_k$	Mult.
ATT [4]	4	2	4	4	4	2
	12	4	8	20	16	5
	28	9				
	20	2				
BLUM [35]	12	4.5	4	1	16	1
	4	0.5	8	14	36	2
	28	4.875				
	44	10.03125				
BLUM-opt [10]	8	1.5	2	0.1875	16	1
	12	2.125	4	0.984	24	1
	40	8.21875				
	32	3.40625				
Alamouti [5]	4	2				
	16	3				
	36	2				
	64	0.5				

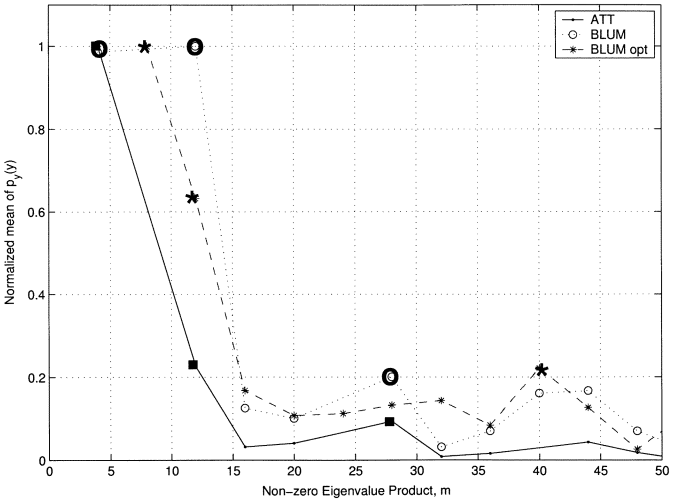

Fig. 5. Normalized $\mathrm{E}\{p_y(y)\} \cdot m^{-1}$ versus measure m for the three 4-state, 4-PSK, two transmit-antenna ST trellis codes. First three dominant measures are indicated in bold type.

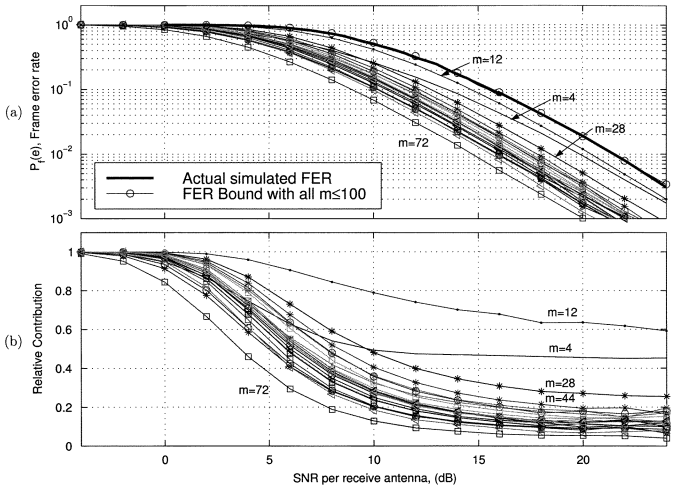

Fig. 6. (a) Bound evaluation of $\mathrm{FER}_m(K)$ for measures $m \in \mathcal{A}, \mathcal{A} = \{4, \ldots, 100\}$ of BLUM code and comparison with both full bound $\mathrm{FER}_{\mathcal{A}}(K)$ and actual FER. (b) Relative contributions of measures $m \in \mathcal{A}$ of BLUM code to full FER bound, $(\mathrm{FER}_m(K))/(\mathrm{FER}_{\mathcal{A}}(K))$. $N = 130$ symbols per frame and one receive antenna.

have similar performance, as noted in the code simulations of Fig. 1. However, when $N = 500$, the ATT code has better performance. We observed similar convergence behavior for two or more receive antennas.

In Fig. 5, we display the predicted dominant quasi-static fading error events of the 4-state, 4-PSK, two transmit-antenna ST trellis codes found in Fig. 2. For each measure m_i from a particular code's measure spectrum, we compute the mean of $p_y(y)$ using the exact PEP expression (5), assuming identical eigenvalues and scaled by h_i/m_i. We use the identical eigenvalue expression, since it upper bounds the mean of $p_y(y)$ for each m_i. As noted in Fig. 5, for low measure error events, we can quickly identify the two to three dominant error events from the measure spectrum. (Note that in Fig. 5, we normalize each plot to the most dominant error event.) We can then rapidly compute the tight bound using only these dominant error events, obtaining a very accurate estimate of the FER for the full range of SNR. These predicted dominant error events are consistent with those identified in Fig. 6(b). We also observe that the dominant events are of low measure, but are not necessarily the lowest measure events. Thus, not surprisingly, multiplicity is an important factor in determining these dominant error events, unlike in the AWGN case.

In Fig. 6(a), we evaluate both $\mathrm{FER}_m(K)$ for each $m \in \mathcal{A}$, and $\mathrm{FER}_{\mathcal{A}}(K)$ for the BLUM 4-PSK trellis code with one receive antenna. Note that $\mathrm{FER}_{\mathcal{A}}(K)$, which is computed with the entire measure spectrum truncated to a maximum measure of 100, accurately estimates the computer simulation of the FER performance over the full range of SNR. We note that if additional measure spectrum elements are incorporated into the bound computation, they do not noticeably increase the bound. The bound, in fact, appears to converge in the measure spectrum to the simulated FER. In addition, we observe that each $\mathrm{FER}_m(K)$ lower bounds the true FER.

In Fig. 6(b), we evaluate the expression $\mathrm{FER}_m(K)/\mathrm{FER}_{\mathcal{A}}(K)$ in order to demonstrate the relative contribution of each determinant $m \in \mathcal{A}$ to the bound. We observe that the zero slope at high SNR indicates that each error-event class achieves the same diversity order as the overall FER upper bound. Fig. 6(b) also exhibits the dominant EEMs with measure 12, 4, and 28. We observe similar dominant EEM behavior with the ATT and BLUM-opt codes (see Table I), as well as in a wide array of published ST trellis and block codes with different numbers of states, numbers of transmit antennas, and modulation alphabets.

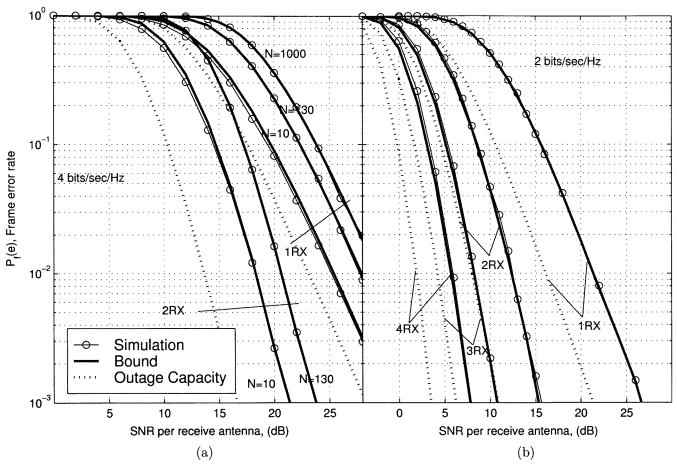

Fig. 7. FER quasi-static fading simulations, improved bounds, and outage capacities. (a) 16-QAM, 4 b/s/Hz Alamouti ST block code for $M = \{1, 2\}$ and $N = \{10, 130, 1000\}$. (b) 4-PSK, 2 b/s/Hz BLUM ST trellis code with $L = 2, M = \{1, 2, 3, 4\}$, and $N = 130$. Only dominant error events $\mathcal{B} = \{12, 4, 28\}$ are used to compute the bounds.

For quasi-static fading, we computed the modified bound for the BLUM 4-PSK ST trellis codes using the dominant error-event set $\mathcal{B} = \{12, 4, 28\}$. Set $\mathcal{B}$, in this case, is ordered according to decreasing dominance, as observed in Fig. 6(b). Only these three error events are required to accurately estimate FER performance over the full range of SNR. In Fig. 7(b), for the BLUM code, we compare the improved bounds with computer

simulations and outage capacity for one, two, three, and four receive antennas and use a frame length of $N = 130$ symbols. All bounds are very accurate over the full range of SNR and are within 2–5 dB of the Gaussian-input outage capacity.

In Fig. 7(a), we plot the performance of the 16-QAM Alamouti code for one and two receive antennas and different frame lengths. We see that the improved bound tracks the reduction in performance as the frame length increases. For $N = 10$, the improved bound is a true upper bound, and tightens as frame length increases.

Further research could provide a mathematical justification for the observed tightness of this FER bound. This convergence behavior with respect to dominant error EEMs over the full range of SNR seems to be a property of the improved bound on the FER, and not of a similarly constructed improved bound on the bit-error rate; see [32].

VI. Conclusion

In this paper, we investigated the accuracy of truncated union bounds on the FER for selected ST trellis and block codes. We developed a general method of computing the *measure spectrum* of ST trellis codes for a variety of channel conditions and number of receive antennas. Traditional ST code design and FER bound analysis using PEPs for quasi-static fading were found to be generally quite loose and nonconvergent in the measure spectrum. We derived a modified bound for the quasi-static fading case, and demonstrated its high accuracy for the full range of SNR. For a selection of ST trellis and block codes, we observed that this improved bound contains *dominant error events* when classified according to their determinant. This numerical bound on the dominant error events provides a rapid method of computing ST code FER performance in quasi-static fading.

References

[1] G. Foschini and M. Cans, "On limits of wireless communications in a fading environment when using multiple antennas," *Wireless Pers. Commun.*, vol. 6, no. 3, pp. 311–334, Mar. 1998.

[2] E. Telatar, "Capacity of multi-antenna Gaussian channels," *Eur. Trans. Telecommun.*, vol. 10, no. 6, pp. 585–596, Dec. 1999.

[3] J. Guey, M. Fitz, M. Bell, and W. Kuo, "Signal design for transmitter diversity wireless communication systems over Rayleigh fading channels," *IEEE Trans. Commun.*, vol. 47, pp. 527–537, Apr. 1999.

[4] V. Tarokh, N. Seshadri, and A. R. Calderbank, "Space–time codes for high-data-rate wireless communication: Performance criterion and code construction," *IEEE Trans. Inform. Theory*, vol. 44, pp. 744–764, Mar. 1998.

[5] S. M. Alamouti, "A simple transmit diversity technique for wireless communications," *IEEE J. Select. Areas Commun.*, vol. 16, pp. 1451–1458, Aug. 1998.

[6] L. Ozarow, S. Shamai, and A. Wyner, "Information theoretic considerations for cellular mobile radio," *IEEE Trans. Veh. Technol.*, vol. 43, pp. 359–378, May 1994.

[7] R. Knopp and P. Humblet, "On coding for block fading channels," *IEEE Trans. Inform. Theory*, vol. 46, pp. 189–205, Jan. 2000.

[8] E. Malkamäki and H. Leib, "Coded diversity on block-fading channels," *IEEE Trans. Inform. Theory*, vol. 45, pp. 771–781, Mar. 1999.

[9] D. M. Ionescu, K. Mukkavilli, Z. Yan, and J. Lilleberg, "Improved 8- and 16-state space-time codes for 4PSK with two transmit antennas," *IEEE Commun. Lett.*, vol. 5, pp. 301–303, July 2001.

[10] Q. Yan and R. Blum, "Optimum space–time convolutional codes," in *Proc. IEEE Wireless Communication, Networking Conf.*, vol. 3, Chicago, IL, Sept. 2000, pp. 1351–1355.

[11] S. Bäro, G. Bauch, and A. Hansmann, "Improved codes for space–time trellis-coded modulation," *IEEE Commun. Lett.*, vol. 4, pp. 20–22, Jan. 2000.

[12] M. Tao and R. Cheng, "Improved design criteria and new trellis code for space–time coded modulation in slow fading channels," *IEEE Commun. Lett.*, vol. 5, pp. 313–315, July 2001.

[13] Z. Chen, B. Vucetic, J. Yuan, and K. Lo, "Space–time trellis codes for 4-PSK with three and four transmit antennas in quasi-static flat fading channels," *IEEE Commun. Lett.*, vol. 6, pp. 67–69, Feb. 2002.

[14] Z. Chen, J. Yuan, and B. Vucetic, "An improved space–time coded modulation scheme on slow Rayleigh fading channels," in *Proc. IEEE Int. Conf. Communications*, vol. 4, Helsinki, Finland, June 2001, pp. 1110–1116.

[15] M. Fitz, J. Grimm, and S. Siwamogsatham, "A new view of performance analysis techniques in correlated Rayleigh fading," in *Proc. IEEE Wireless Communication, Networking Conf.*, vol. 1, New Orleans, LA, Sept. 1999, pp. 139–144.

[16] A. P. des Rosiers and P. H. Siegel, "On performance bounds for space–time coded modulation on fading channels," in *Proc. Int. Symp. Information Theory and Its Applications*, vol. 2, Honolulu, HI, Nov. 2000, pp. 496–472.

[17] E. Biglieri, G. Taricco, and A. Tulino, "Performance of space–time codes for a large number of antennas," *IEEE Trans. Inform. Theory*, vol. 48, pp. 1794–1803, July 2002.

[18] G. Taricco and E. Biglieri, "Exact pairwise error probability of space–time codes," *IEEE Trans. Inform. Theory*, vol. 48, pp. 510–513, Feb. 2002.

[19] M. Uysal and C. Georghiades, "On the error performance analysis of space–time trellis codes: An analytical framework," in *Proc. IEEE Wireless Communication, Networking Conf.*, vol. 1, Orlando, FL, Mar. 2002, pp. 99–104.

[20] S. Benedetto, M. Mondin, and G. Montorsi, "Performance evaluation of trellis-coded modulation schemes," *Proc. IEEE*, vol. 82, pp. 833–855, June 1994.

[21] D. Aktas and M. Fitz, "Distance spectrum of space–time trellis-coded modulations in quasi-static Rayleigh fading channels," *IEEE Trans. Inform. Theory*, vol. 49, pp. 3335–3344, Dec. 2003.

[22] S. Siwamogsatham, M. Fitz, and J. Grimm, "A new view of performance analysis of transmit diversity schemes in correlated Rayleigh fading," *IEEE Trans. Inform. Theory*, vol. 48, pp. 950–956, Apr. 2002.

[23] E. Malkamäki and H. Leib, "Evaluating the performance of convolutional codes over block fading channels," *IEEE Trans. Inform. Theory*, vol. 45, pp. 1643–1646, July 1999.

[24] H. Bouzekri and S. Miller, "Analytical tools for space–time codes over quasi-static fading channels," in *Proc. IEEE Int. Conf. Communications*, vol. 3, New York, NY, Apr. 2002, pp. 1377–1381.

[25] M. Byun, D. Park, and B. Lee, "Performance analysis of space–time trellis-coded modulation in quasi-static Rayleigh fading channels," in *Proc. IEEE Int. Conf. Communications*, vol. 3, New York, NY, Apr. 2002, pp. 1596–1600.

[26] A. Stefanov and T. Duman, "Performance bounds for space–time trellis codes," *IEEE Trans. Inform. Theory*, vol. 49, pp. 2134–2140, Sept. 2003.

[27] A. P. des Rosiers and P. H. Siegel, "Space–time code performance bounds on quasi-static fading channels," in *Proc. IEEE Int. Conf. Communications*, vol. 5, Anchorage, AK, May 2003, pp. 3160–3164.

[28] A. Viterbi and J. Omura, *Principles of Digital Communication and Coding*. New York: McGraw-Hill, 1979.

[29] J. Proakis, *Digital Communications*, 3rd ed. New York: McGraw-Hill, 1995.

[30] D. M. Ionescu, "On space–time code design," *IEEE Trans. Wireless Commun.*, vol. 2, pp. 20–28, Jan. 2003.

[31] S. S. Pietrobon, "On the probability of error of convolutional codes," *IEEE Trans. Inform. Theory*, vol. 42, pp. 1562–1568, Sept. 1996.

[32] A. P. des Rosiers, "The theory and practice of space–time coding," Ph.D. dissertation, Univ. California, San Diego, La Jolla, CA, 2004.

[33] V. Tarokh, H. Jafarkhani, and A. R. Calderbank, "Space–time block codes from orthogonal design," *IEEE Trans. Inform. Theory*, vol. 45, pp. 1456–1467, July 1999.

[34] G. Bauch and J. Hagenauer, "Analytical evaluation of space–time transmit diversity with FEC coding," in *Proc. IEEE Global Telecommunications Conf.*, vol. 1, San Antonio, TX, Nov. 2001, pp. 435–439.

[35] R. Blum, "New analytical tools for designing space–time convolutional codes," in *Proc. Conf. Information Sciences, Systems*, Princeton, NJ, Mar. 2000, pp. WP3-1–WP3-6.

[36] R. Horn and C. Johnson, *Matrix Analysis*. Cambridge, U.K.: Cambridge Univ. Press, 1996.

André P. des Rosiers received the B.S. in electrical engineering from the University of Virginia, Charlottesville, VA, and the M.S. degree from the University of California, San Diego, La Jolla, where he is currently working toward the Ph.D. degree in electrical and computer engineering.

In 2003, he joined the Research Staff of the Adaptive Processing Section, Radar Division, Naval Research Laboratory, Washington, DC, where he is engaged in research in synthetic aperture radar, multiple sensor data analysis, space–time coding, and adaptive signal processing.

Paul H. Siegel (M'82–SM'90–F'97) received the S.B. degree in 1975 and the Ph.D. degree in 1979, both in mathematics, from the Massachusetts Institute of Technology, Cambridge.

He was with the IBM Research Division from 1980 to 1995. He joined the Faculty of the School of Engineering, University of California, San Diego, in July, 1995, where he is currently Professor of Electrical and Computer Engineering. He is affiliated with the Center for Wireless Communications and became Director of the Center for Magnetic Recording Research in September, 2000. His primary research interest is the mathematical foundations of signal processing and coding, especially as applicable to digital data storage and communications. He holds several patents in the area of coding and detection for digital recording systems.

Dr. Siegel was a corecipient of the 1992 IEEE Information Theory Society Paper Award and the 1993 IEEE Communications Society Leonard G. Abraham Prize Paper Award. He held a Chaim Weizmann Fellowship during a year of postdoctoral study at the Courant Institute, New York University, New York. He was a member of the Board of Governors of the IEEE Information Theory Society from 1991 to 1996. He served as Co-Guest Editor of the May 1991 Special Issue on Coding for Storage Devices of the IEEE TRANSACTIONS ON INFORMATION THEORY, of which he is currently Editor-in-Chief, and was an Associate Editor for Coding Techniques from 1992 to 1995. He is a member of Phi Beta Kappa.